

Dear Hal Maring,

We have carefully read the additional comments made by Reviewer 2, and have prepared the following answer and the changes are reflected in the attached revised manuscript.

### **Answers to comments from Referee #2**

**1. Abstract (line 8). 0.56 ppm in XCO<sub>2</sub> is not a small bias. In fact this bias alone would consume the entire error budget of TCCON. In fact, site-to-site bias of 0.56 ppm would essentially render TCCON useless for most carbon cycle science. The precision requirements described (Rayner and OBrien; Olsen and Randerson) refer to bias-free measurement precision and so are not relevant to the discussion here where a one hour average of the FTS data will have essentially negligibly small random precision. Given the uncertainty in the cause of the bias between the two beamsplitters, it isnt clear how it could be homogenized without extensive and ongoing characterization. In summary, I think this study rather than confirming that KBr beamsplitter is acceptable offers significant evidence that this option should be approached cautiously.**

We agree with this comment and removed the word "small" in line 8 of the abstract. Part of the next sentence was also left out "...and could be taken into account when homogenizing or comparing data from both beamsplitters".

The sentence "For the homogenization ..." that starts in line 188 was also removed.

We realize that this bias in not insignificant and should be treated cautiously.

**2. I continue to object to the comparison between the diurnal changes in XCO<sub>2</sub> shown here and in situ measurements from MLO. This makes absolutely no sense and the implication that this comparison gives confidence in the XCO<sub>2</sub> diurnal signal is ill advised. What is the flux implied by the changes in XCO<sub>2</sub>? Answer: huge! I urge the authors to scrub this from the manuscript. Fine to show the diurnal figure, but I believe that the changes shown are (largely) just evidence for airmass bias. A plot of XCO<sub>2</sub> vs airmass (which should certainly be included) would illustrate that the majority of the diurnal signal is associated with airmass rather than time of day (as would be expected from a flux).**

We followed the recommendation and removed Figure 10 and replaced it with another one showing the dependence of our measurements with the SZA. The text was adapted as followed:

Removed the sentence in lines 199 to 201 and replaced it with the following text:

"In Figure 10, we present the XCO<sub>2</sub> and seasonally detrended XCO<sub>2</sub> averages showing a clear dependence with respect to the solar zenith angle."

The following argument was added to denote a large CO<sub>2</sub> diurnal variability observed in in situ data and its implications to the SZA dependence:

"However, a quantitative analysis correlating these observations with in situ measurements at Alzomoni, with a night-to-day average amplitude of approximately 5 ppm, indicates that carbon capture processes can be contributing significantly to the shown SZA dependence".

Finally, the sentence in lines 208 to 211 was removed "For comparison, ..."

**3. What is the basis for the final sentence: This data set confirms a small influence of anthropogenic emissions especially during the afternoon, when the regional boundary layer reaches the height of the station.? A figure of XCO might offer some evidence for this, but that is not discussed or shown.**

The second part of the sentence and next sentence in lines 237 to 239 was completely removed: "..., while the mean diurnal pattern reflects a decrease of up to 1.5 ppm during sunlit hours. This data set confirms a small influence of anthropogenic emissions especially during the afternoon, when the regional boundary layer reaches the height of the station".

## Errata

"Intercomparision" in line 50 was corrected to "intercomparison"

"weren't" in line 168 was corrected to "were not"

The sentence that begins in line 184, that reads "The bias for CO<sub>2</sub> column was calculated from the biases obtained above ( $\Delta$ XCO<sub>2</sub> and O<sub>2</sub>  $\Delta$ O<sub>2</sub>) using ..." should read "The bias for CO<sub>2</sub> column was calculated from the biases obtained above ( $\Delta$ XCO<sub>2</sub> and  $\Delta$ O<sub>2</sub>) using ...".

"Remaines" in line 219 was corrected to "remains"

"beamsplktters" in line 223 was corrected to "beamsplitters"

The first sentence of the Figure 5 caption ends with "... obtained from the top-down approach." but should end with "... obtained from the Section 3.2 approach." In the second sentence of the same caption the word "precisin" was corrected to "precision".

# Background CO<sub>2</sub> levels and error analysis from ground-based solar absorption IR measurements in central Mexico

Jorge L. Baylon<sup>1</sup>, Wolfgang Stremme<sup>1</sup>, Michel Grutter<sup>1</sup>, Frank Hase<sup>2</sup>, and Thomas Blumenstock<sup>2</sup>

<sup>1</sup>Centro de Ciencias de la Atmósfera, Universidad Nacional Autónoma de México, Mexico

<sup>2</sup>Institute of Meteorology and Climate Research, Karlsruhe Institute of Technology, Germany

Correspondence to: (baylon@atmosfera.unam.mx)

**Abstract.** In this investigation we analyze two common optical configurations to retrieve CO<sub>2</sub> total column amounts from solar absorption infrared spectra. The noise errors using either a KBr or a CaF<sub>2</sub> beamsplitter, a main component of a Fourier transform infrared (FTIR) spectrometer, are quantified in order to assess the relative precisions of the measurements. The configuration using a CaF<sub>2</sub> beamsplitter, as deployed by the instruments which contribute to the Total Carbon Column Observing Network (TCCON), shows a slightly better precision. However, we show that the precisions in  $X_{CO_2}$  ( $= 0.2095 \cdot \frac{\text{Total Column } CO_2}{\text{Total Column } O_2}$ ) retrieved from >96% of the spectra measured with a KBr beamsplitter, fall well below 0.2%. A **small**-bias in  $X_{CO_2}$  (KBr - CaF<sub>2</sub>) of  $+0.56 \pm 0.25$  ppm was found when using an independent data set as reference. This value, which corresponds to  $+0.14 \pm 0.064$  %, is slightly larger than the mean precisions obtained ~~and could be taken into account when homogenizing or comparing data from both beamsplitters~~. A 3-year  $X_{CO_2}$  time series from FTIR measurements at the high-altitude site of Altzomoni in central Mexico presents clear annual and diurnal cycles and a trend of  $+2.2$  ppm/yr could be determined.

## 1 Introduction

During the last decades, carbon dioxide (CO<sub>2</sub>) has exceeded the pre-industrial levels by about 40% mainly due to fossil fuel combustion and land use change (Hartmann et al., 2013), contributing more than any other anthropogenic gas to the positive total radiative forcing of the Earth and becoming the most important anthropogenic greenhouse gas (Myhre et al., 2013). The quantification of the spatial distribution and temporal variation of CO<sub>2</sub> sources and sinks can help to understand the anthropogenic contributions of CO<sub>2</sub> to the carbon cycle. This task can be achieved by monitoring the atmosphere using ground-based and satellite observations. Ground-based networks like the Global Atmospheric Watch WMO (2014) or the Total Column Carbon Observing Network (TCCON) provide data sets of CO<sub>2</sub> concentrations around the world. TCCON is a network of Fourier transform

infrared spectrometers that record solar absorption spectra in the near infrared (NIR, 3,300-13,000  
25  $\text{cm}^{-1}$ ) spectral region in order to retrieve column-averaged dry-air mole fractions of  $\text{CO}_2$  ( $X_{\text{CO}_2}$ )  
and other molecules that absorb in the NIR (Wunch et al., 2011). TCCON aims to provide reliable,  
long-term validation data sets for satellite measurements and to improve current knowledge of the  
carbon cycle. Measurements of  $\text{CO}_2$  from space have been done by many satellite missions like ACE  
(Foucher et al., 2011), AIRS (Chahine et al., 2008), IASI (Crevoisier et al., 2009), TES (Kulawik  
30 et al., 2010), SCIAMACHY (Reuter et al., 2011), GOSAT (Kuze et al., 2009) and OCO-2 (Wunch  
et al., 2016) with the last three missions relying on TCCON data for validation.

Studies done to estimate the  $\text{CO}_2$  concentrations in Mexico City and central Mexico have been  
scarce, the first one was conducted during 1981 and 1982 in which the diurnal and seasonal variation  
was estimated taking air samples in different parts of the city (Báez et al., 1988). In two different  
35 campaigns (MCMA-2003 and MILAGRO) the  $\text{CO}_2$  fluxes and concentrations during typical days in  
the Mexico City Metropolitan Area (MCMA) were estimated using the eddy covariance technique  
(Velasco et al., 2005, 2009). The first study using a FTS was done during September 2001 in the  
south of the MCMA using a Nicolet Nexus interferometer with a resolution of  $0.125 \text{ cm}^{-1}$  and  
retrieving  $\text{CO}_2$  in the  $723\text{-}766 \text{ cm}^{-1}$  spectral region (Grutter, 2003). From this study the variability  
40 and average diurnal cycle of  $\text{CO}_2$  was recorded with high temporal resolution.

The Alzomoni site is located to the southeast of the MCMA at a height of almost 4,000 m above  
the sea level. Measurements of NIR and MIR spectra have been conducted since 2012 using a Bruker  
IFS 120/5 HR. The site is part of the NDACC network since 2015 and has been reporting vertical  
columns of  $\text{O}_3$ ,  $\text{CO}$ ,  $\text{N}_2\text{O}$  and  $\text{CH}_4$  among other gases. As part of the NDACC instrumental config-  
45 uration, a KBr beamsplitter has been used for most of the measurements but for a limited number of  
days, a  $\text{CaF}_2$  beamsplitter was also used in order to meet the TCCON instrumental requirements and  
compare the effect of each configuration in the retrievals of  $\text{CO}_2$ ,  $\text{O}_2$  as well as in the estimation of  
 $X_{\text{CO}_2}$ .

This paper presents  $X_{\text{CO}_2}$  retrieved from NIR spectra measured from December 2012 to Decem-  
50 ber 2015 in the Alzomoni site and an ~~intereomparision~~ intercomparison of how the use of KBr and  
 $\text{CaF}_2$  beamsplitters affect the errors and precision of  $\text{CO}_2$ ,  $\text{O}_2$  columns and  $X_{\text{CO}_2}$  mole fractions.  
Section 2 describes the configuration used in the measurement of the NIR spectra and how these  
spectra were analyzed for producing the time series of  $X_{\text{CO}_2}$ . An evaluation of how the used beam-  
splitter influence the total column retrievals and the calculation of  $X_{\text{CO}_2}$  by means of an estimation  
55 of noise errors, precision and bias of each configuration is presented in Sect. 3. The characteristic  
seasonal and diurnal cycles, as well as the observed trend for this sub-tropical site in central Mexico,  
are presented in Sect. 4.

## 2 FTIR instrument, measurement site and spectral analysis

A high resolution Fourier Transform InfraRed (FTIR) spectrometer, Bruker model HR 120/5, was  
60 deployed to measure solar absorption spectra under clear sky conditions. The instrument began op-  
erations at a high-altitude location in central Mexico in 2012 as part of a collaboration between the  
National Autonomous University of Mexico (UNAM) and the Karlsruhe Institute of Technology  
(KIT) and since 2015, Altzomoni has been part of the Network for the Detection of Atmospheric  
Composition Change (NDACC). Routine and remotely-operated measurements are performed with  
65 a spectral resolution of  $0.005\text{ cm}^{-1}$  using a KBr beamsplitter, a set of band-pass filters and liquid-  
nitrogen cooled MCT and InSb detectors, according to NDACC specifications. The solar tracking is  
based on the Camtracker system (Gisi et al., 2011) used in other NDACC and TCCON sites and is  
housed in a dome which can be operated remotely.

Alternatively, an InGaAs detector is used to record near-infrared (NIR) spectra within each mea-  
70 surement sequence with a resolution of  $0.02\text{ cm}^{-1}$ . These NIR spectra, used in this study to retrieve  
 $\text{CO}_2$  and  $\text{O}_2$ , were recorded as the average of 2 scans taking approximately 38 seconds with a scan-  
ner speed of 40 kHz. In each measurement sequence, a set of six NIR measurements are recorded,  
taking around 5 minutes. This small change in solar angles allow the consideration that all measure-  
ments belong to the same airmass. A  $\text{CaF}_2$  beamsplitter is also available and was used for a small  
75 number of days for the purpose of estimating the noise levels in each optical configuration and how  
this affects the retrievals.

The FTIR instrument is located at the Altzomoni high-altitude station ( $19.1187^\circ\text{N}$ ,  $98.6552^\circ\text{W}$ )  
located in central Mexico within the Izta-Popo National Park, 60 km southeast of Mexico City, at an  
altitude of 3,985 m a.s.l. This station is part of the University Network of Atmospheric Observatories  
80 ([www.ruoa.unam.mx](http://www.ruoa.unam.mx)) and comprises a complete set of in situ and meteorological instrumentation.

The measured spectra were analyzed with the retrieval code PROFFIT which uses the radiative  
transfer code PROFFWD (Hase et al., 2004). For the calculation of the dry-air column-average mole  
fractions of carbon dioxide  $X_{\text{CO}_2}$ ,  $\text{CO}_2$  and  $\text{O}_2$  were retrieved separately using a profile scaling  
procedure and with the microwindows and interfering species listed in Table 1. Pressure and tem-  
85 perature profiles from the National Center for Environment Prediction (NCEP) were used and the a  
priori profiles were obtained from the Whole Atmosphere Community Climate Model (WACCM).  
A single a priori profile of each retrieved species was used for the entire set of measurements.

## 3 Effect of the beamsplitter on the retrieval

The TCCON instrumental requirements state that the network's necessary precision is best achieved  
90 using a  $\text{CaF}_2$  beamsplitter (TCCON-Wiki), but in the case of the Altzomoni site, this would mean  
sacrificing routine measurements of spectra in the mid-infrared (MIR,  $200\text{-}3,300\text{ cm}^{-1}$ ) region since  
the beamsplitter change needs to be performed manually. Given the location of the site and aside

from complying with a long term commitment with NDACC, it is of great interest to perform measurements of gases which absorb in the MIR region in order to characterize pollution transport events in the region and study the composition of the gases emitted by the active Popocatepetl volcano. For these reasons, a KBr beamsplitter has been part of the configuration used in the site and the use of the CaF<sub>2</sub> beamsplitter has been limited. Figure 1 shows two tungsten NIR lamp spectra, one measured with KBr (red) and another one with CaF<sub>2</sub> (blue) to illustrate the features of each measurement in the NIR region. The KBr spectra shows a slightly lower intensity and a dip on the 5000-6000 cm<sup>-1</sup> spectral region. Kiel et al. (2016) showed that a small curvature might affect the retrieval results if no baseline is adjusted. The settings used for the retrievals of this study adjusted a smoothed baseline with 20 parameters for each microwindow used. The baseline curvature in the spectral region around the dip introduced by the KBr beamsplitter is removed using a simplified radiometric calibration, assuming that the tungsten lamp produces a blackbody spectrum (T=1700 K) and that there is no self-emission of the optical set-up in the spectral region above 4000 cm<sup>-1</sup>. This calibration has a low impact on the columns (+0.021% CO<sub>2</sub>, +0.0053% for O<sub>2</sub>) due to the simultaneous fit of the baseline in the retrieval code.

In order to compare the impact of the KBr and CaF<sub>2</sub> beamsplitters on the retrievals and since far more measurements are available with the KBr beamsplitter (27,148) than with CaF<sub>2</sub> (2,093), an ensemble of KBr measurements was formed reproducing the size and solar zenith angle (SZA) distribution of the CaF<sub>2</sub> measurements. A condition imposed was to only consider sets of consecutive measurements done within a five minute lapse so that the precision of each retrieval product and SZA could be calculated. As shown in Fig. 2, the KBr ensemble consisted in measurements from 101 days between July 30, 2013 and December 30, 2015 while the CaF<sub>2</sub> ensemble had measurement from 43 days from February 15, 2014 to June 23, 2015.

For the case of CO<sub>2</sub> column measurements, two references of precision exist: Rayner and O'Brien (2001) showed that a 0.25% network precision would improve the current knowledge of the carbon cycle while Olsen and Randerson (2004) suggested that a 0.1% precision would allow an assessment of the strength of the carbon sink in the Northern Hemisphere. The following sub-sections are dedicated to determining where the Alzomoni data fall, using routinely a KBr beamsplitter, in terms of these two benchmarks.

### 3.1 Retrieved CO<sub>2</sub> and O<sub>2</sub> error budgets

The error calculation implemented in PROFFIT allows one to estimate the errors associated with a total column retrieval (Barthlott et al., 2015). These include channelling and offset, instrumental line shape (ILS), temperature profile, line-of-sight (LOS), solar lines, spectroscopy and noise errors. The errors were calculated for each of the measurements that comprise the KBr and CaF<sub>2</sub> ensembles. The magnitude of the uncertainties and the statistical and systematic contributions for each source are listed in Table 2. The largest error difference between beamsplitters is expected to originate from

the noise for a given ensemble, since the spectral windows used for the retrievals are measured with  
 130 a different signal/noise ratios (see Fig. 1). The purpose of obtaining the errors from the PROFFIT  
 software was to determine the value of noise present in each measurement and how it depends on  
 the beamsplitter used. The noise calculation from PROFFIT takes into account the derivatives of  
 the retrieval with respect of the measurement and the difference between the measurement and a  
 simulated spectra from the forward model. Figures 3 and 4 show how the mean noise error from  
 135 the CO<sub>2</sub> and the O<sub>2</sub> total columns depend on the beamsplitter and the SZA, while Tables 3 and 4  
 show the mean values of each error source for two SZA values (20 and 70°). The noise error of  
 the CO<sub>2</sub> column shows good agreement between beamsplitters for SZA's above 30°, but is lower in  
 KBr measurements at smaller angles. For the O<sub>2</sub> column, the errors have similar behavior for angles  
 below 30°, but the noise errors for angles above this value remain more or less constant and are  
 140 30 - 40 % larger for KBr than for CaF<sub>2</sub>. Overall, the total statistical and systematic errors for both  
 beamsplitters estimated with this technique are quite similar.

### 3.2 Statistical precision from consecutive measurements

For a statistical estimation of the precision, we consider that the standard deviation of the consecutive  
 measurements done within a 5-minute lapse (typically 6 spectra) represents the overall precision of  
 145 the measurements. This method is based on the assumption that the actual gas columns undergo  
 smaller changes in the short time considered than the measurement error. With the three products  
 derived from a NIR measurement (CO<sub>2</sub> and O<sub>2</sub> columns and X<sub>CO<sub>2</sub></sub>), three different precisions were  
 calculated and used for estimating which part of the random error is independent from the CO<sub>2</sub> and  
 O<sub>2</sub> columns and which part is correlated and thus cancels out when the X<sub>CO<sub>2</sub></sub> ratio is calculated.

150 Assuming that the precisions of CO<sub>2</sub> and O<sub>2</sub> ( $\sigma_{CO_2}$  and  $\sigma_{O_2}$ ) are due to both the noise and the  
 correlated errors (see Eq. 1&2), and the precision of X<sub>CO<sub>2</sub></sub> depends only in the noise from both  
 columns (Eq. 3), a system of equations was formed and solved using the mean precisions of the  
 three products to obtain the mean correlated and noise errors of CO<sub>2</sub> and O<sub>2</sub> for each beamsplitter.

$$(\sigma_{CO_2})^2 = (\sigma^{Correlated})^2 + (\sigma_{CO_2}^{Noise})^2 \quad (1)$$

$$155 \quad (\sigma_{O_2})^2 = (\sigma^{Correlated})^2 + (\sigma_{O_2}^{Noise})^2 \quad (2)$$

$$(\sigma_{X_{CO_2}})^2 = (\sigma_{CO_2}^{Noise})^2 + (\sigma_{O_2}^{Noise})^2 \quad (3)$$

As can be seen in the results from this exercise presented in Table 5, the mean noise errors from  
 the columns are within the range of the values obtained using PROFFIT and in the case of X<sub>CO<sub>2</sub></sub>,  
 the mean value from all the KBr measurements in the ensemble was 25% higher than with CaF<sub>2</sub>.  
 160 The contribution appears to be dominated by the noise in the O<sub>2</sub> retrieval. This is in accordance to  
 the result in Sect. 3.1. However as Figure 5 shows, the mean X<sub>CO<sub>2</sub></sub> precisions obtained from both  
 beamsplitters were below 0.1% and those of >96% of all the spectra in the ensemble measured with  
 a KBr beamsplitter, fall below the 0.2% value.

### 3.3 Bias estimation

165 The systematic difference between beamsplitters was estimated for the three products obtained. Since there are no temporal coincidences between the measurements with both beamsplitters, an independent set of measurements was used to calculate the bias. The ensembles were sorted in bins, so that the mean values of the data in each bin could be compared even if the measurements on the ensembles ~~weren't~~ were not coincident in time.

170 For  $X_{CO_2}$ , the continuous data set of  $CO_2$  in situ measurements from the Mauna Loa Observatory (MLO; 19.5362°N, 155.5763°W, 3,397 m.a.s.l) was chosen, given the fact that both sites share a similar latitude and altitude. An in situ measurement in Alzomoni is now available but the data does not cover the entire period of the FTIR ensemble. Although both data sets show a similar behavior, the intention of using MLO in this context was to investigate the relative bias between  
175 both beamsplitters ensembles with a common reference by arranging the data into bins. There were 189 coincidences for the KBr and 174 for  $CaF_2$  data sets. The bias was obtained from the mean of the KBr– $CaF_2$  differences of these coincidences, sorted in 13 bins generated using the measurements in MLO. From the correlation plot for each beamsplitter and a Bland-Altman plot (Bland and Altman, 1986) for their differences shown in Figure 7, a bias of  $+0.14 \pm 0.064 \%$  is obtained for  $X_{CO_2}$ .

180 In the case of  $O_2$  total columns, a bias was calculated by estimating the dry pressure column from surface pressure measurements at Alzomoni and the  $H_2O$  total columns retrieved in the NIR spectral region, which in turn was multiplied by the factor 0.2095 to convert to  $O_2$  column. The number of coincidences obtained between the data sets was 100 for KBr and 110 for  $CaF_2$ . Figure 8 shows the plots and KBr– $CaF_2$  differences resulting in a bias of  $-0.17 \pm 0.029 \%$ .

185 The bias for  $CO_2$  column was calculated from the biases obtained above ( $\Delta X_{CO_2}$  and  $\Theta_2 \Delta O_2$ ) using Eq. 4:

$$\Delta X_{CO_2} = \frac{\partial X_{CO_2}}{\partial CO_2} \cdot \Delta CO_2 + \frac{\partial X_{CO_2}}{\partial O_2} \cdot \Delta O_2, \quad (4)$$

from which a value of  $\Delta CO_2 = -0.030 \pm 0.070 \%$  is obtained. The biases and the mean values for each beamsplitter are summarized in Table 6. ~~For the homogenization of a data set, the relative~~

190  ~~$X_{CO_2}$  bias between beamsplitters can be corrected by multiplying the KBr data by the factor 0.9986.~~

### 4 Observed time series

Figure 9 shows the daily means of the  $X_{CO_2}$  in black, derived from 29,241 measurements done in Alzomoni during 510 days between December 28, 2012 and December 30, 2015. A function was  
195 adjusted to the data using Eq. 5, taken from Wunch et al. (2013), where  $x$  is the decimal year and the obtained fitting parameters were as follows:  $\alpha = 2.19 \text{ ppm yr}^{-1}$ ,  $a_0 = -0.0040 \text{ ppm}$ ,  $a_1 = -0.93 \text{ ppm}$ ,  $a_2 = 0.95 \text{ ppm}$ ,  $b_1 = 1.60 \text{ ppm}$ ,  $b_2 = -0.54 \text{ ppm}$ . The linear term determines the trend of the

series which has the value of 2.2 ppm/year. The same function fitted over the MLO data set shows also a 2.2 ppm/year trend.

$$f(x) = \alpha x + \sum_{k=0}^2 a_k \cos(2\pi kx) + b_k \sin(2\pi kx). \quad (5)$$

The daily average mixing ratio from all the FTIR data is presented in Figure 10. These hourly data were detrended using the fitted curve obtained for the annual cycle and the local time was converted to true solar time in order to observe the distinct effect of vegetation. In Figure 10, we present the  $X_{CO_2}$  and seasonally detrended  $X_{CO_2}$  averages showing a clear dependence with respect to the solar zenith angle. Although a treatment of the airmass dependence for  $X_{CO_2}$  has been considered following Dohe (2013) and Kiel et al. (2016), this may still not be fully corrected in the reported  $X_{CO_2}$ . However, a qualitative-quantitative analysis correlating these observations with in situ measurements indicate at Altzomoni, with a night-to-day average amplitude of approximately 5 ppm, indicates that carbon capture and transport processes are responsible for most of the diurnal variability observed over the Altzomoni site. processes can be contributing significantly to the shown SZA dependence. The weekday averages were also calculated and no distinct weekly pattern was detected from these data which indicates that the measurements are representative for the free atmosphere and the influence of the nearby cities are minimal with respect to the total column. For comparison, the detrended diurnal cycle of the MLO data is also shown in the figure and despite that it is at a different location and corresponds to in situ measurements, it shows a similar behavior with a smaller amplitude and a minimum which occurs 3 hours later.

## 5 Conclusions

Solar absorption FTIR measurements done with KBr and CaF<sub>2</sub> beamsplitters were compared using equivalent ensembles containing more than 2 thousand spectra. The two methods used for evaluating the statistical errors gave similar results. In the case of CO<sub>2</sub> columns, the noise levels from the KBr measurements are on average 20% lower than from CaF<sub>2</sub> measurements when solar zenith angles are below 30°. Measurements with larger SZA's have similar errors with both beamsplitters. Larger error differences are encountered from the O<sub>2</sub> column retrievals. For angles below 30° the noise in KBr measurements is around 29% lower but increases with the angle and remains remains constant above the CaF<sub>2</sub> levels, approximately 38% higher.

Thus, in this study an estimation of the precision of each ensemble shows that the largest statistical error contribution in  $X_{CO_2}$  comes from the O<sub>2</sub> column retrieval. This outcome has the implication that column averaged mixing ratios retrieved using KBr beamsplitters beamsplitters have noise-related errors which are on average about 25% larger than with CaF<sub>2</sub>. However, mean  $X_{CO_2}$  precisions was found to be below 0.1% and >96% of the measurements made with both optical configurations fall well below the 0.2% precision.

These results provide enough evidence that measurements performed with a KBr beamsplitters are reliable and useful for carbon cycle studies. This includes all FTIR instruments which are committed to comply with NDACC requirements and have an additional InGaAs detector available for NIR  
235 spectral measurements. A larger number of sites producing confident  $X_{CO_2}$  data sets would allow to increase our current knowledge of the variability of this important greenhouse gas.

When doing direct comparisons across a network or using single retrievals for intercomparing timed observations, however, one needs to be cautious and consider a possible bias. We have estimated a bias of 0.14% for  $X_{CO_2}$  between beamsplitters using data from the Mauna Loa Observatory.

240 A rich data set of  $X_{CO_2}$  was put together from more than 3 years of measurements in central Mexico. A very distinct annual cycle was identified with an amplitude of ~6 ppm and a positive trend of 2.2 ppm/year, ~~while the mean diurnal pattern reflects a decrease of up to ~1.5 ppm during sunlit hours. This data set confirms a small influence of anthropogenic emissions especially during the afternoon, when the regional boundary layer reaches the height of the station.~~

245 *Acknowledgements.* We would like to thank the financial support from UNAM-DGAPA (IN109914 & IN112216) and CONACYT (0249374 & 0239618). JB received a full stipend from CONACYT throughout his PhD work as well as financial support from UNAM's Earth Sciences Graduate Program. The Mauna Loa Observatory and the RUOA Network (Red Universitaria de Observatorios Atmosféricos – UNAM) are acknowledged for making the in situ measurements available. Special thanks go to Alejandro Bezanilla, Maria Eugenia González, Delibes  
250 Flores, Héctor Soto and Omar López for their technical support in this investigation.

## References

- Báez, A., Reyes, M., Rosas, I., and Mosino, P.: CO<sub>2</sub> concentrations in the highly polluted atmosphere of Mexico City, *Atmósfera*, 1, <http://www.revistascca.unam.mx/atm/index.php/atm/article/view/8271>, 1988.
- Barthlott, S., Schneider, M., Hase, F., Wiegeler, A., Christner, E., González, Y., Blumenstock, T., Dohe, S.,  
255 García, O. E., Sepúlveda, E., Strong, K., Mendonca, J., Weaver, D., Palm, M., Deutscher, N. M., Warneke, T., Notholt, J., Lejeune, B., Mahieu, E., Jones, N., Griffith, D. W. T., Velasco, V. A., Smale, D., Robinson, J., Kivi, R., Heikkinen, P., and Raffalski, U.: Using XCO<sub>2</sub> retrievals for assessing the long-term consistency of NDACC/FTIR data sets, *Atmospheric Measurement Techniques*, 8, 1555–1573, doi:10.5194/amt-8-1555-2015, <http://www.atmos-meas-tech.net/8/1555/2015/>, 2015.
- 260 Bland, J. M. and Altman, D.: STATISTICAL METHODS FOR ASSESSING AGREEMENT BETWEEN TWO METHODS OF CLINICAL MEASUREMENT, *The Lancet*, 327, 307 – 310, doi:[http://dx.doi.org/10.1016/S0140-6736\(86\)90837-8](http://dx.doi.org/10.1016/S0140-6736(86)90837-8), <http://www.sciencedirect.com/science/article/pii/S0140673686908378>, 1986.
- Chahine, M. T., Chen, L., Dimotakis, P., Jiang, X., Li, Q., Olsen, E. T., Pagano, T., Randerson, J., and  
265 Yung, Y. L.: Satellite remote sounding of mid-tropospheric CO<sub>2</sub>, *Geophysical Research Letters*, 35, doi:10.1029/2008GL035022, <http://dx.doi.org/10.1029/2008GL035022>, 117807, 2008.
- Crevoisier, C., Chédin, A., Matusueda, H., Machida, T., Armante, R., and Scott, N. A.: First year of upper tropospheric integrated content of CO<sub>2</sub> from IASI hyperspectral infrared observations, *Atmospheric Chemistry and Physics*, 9, 4797–4810, doi:10.5194/acp-9-4797-2009, <http://www.atmos-chem-phys.net/9/4797/2009/>,  
270 2009.
- Dohe, S.: Measurements of atmospheric CO<sub>2</sub> columns using ground-based FTIR spectra, Ph.D. thesis, Karlsruhe Institut für Technologie (KIT), 2013.
- Foucher, P. Y., Chédin, A., Armante, R., Boone, C., Crevoisier, C., and Bernath, P.: Carbon dioxide atmospheric vertical profiles retrieved from space observation using ACE-FTS solar occultation instrument, *Atmospheric  
275 Chemistry and Physics*, 11, 2455–2470, doi:10.5194/acp-11-2455-2011, <http://www.atmos-chem-phys.net/11/2455/2011/>, 2011.
- Gisi, M., Hase, F., Dohe, S., and Blumenstock, T.: Camtracker: a new camera controlled high precision solar tracker system for FTIR-spectrometers, *Atmospheric Measurement Techniques*, 4, 47–54, doi:10.5194/amt-4-47-2011, <http://www.atmos-meas-tech.net/4/47/2011/>, 2011.
- 280 Grutter, M.: Multi-Gas analysis of ambient air using FTIR spectroscopy over Mexico City, *Atmósfera*, 16, <http://www.revistascca.unam.mx/atm/index.php/atm/article/view/8506>, 2003.
- Hartmann, D., Klein Tank, A., Rusticucci, M., Alexander, L., Brönnimann, S., Charabi, Y., Dentener, F., Dlugokencky, E., Easterling, D., Kaplan, A., Soden, B., Thorne, P., Wild, M., and Zhai, P.: Observations: Atmosphere and Surface, in: *Climate Change 2013: The Physical Science Basis. Contribution of Working Group I to the Fifth Assessment Report of the Intergovernmental Panel on Climate Change*, edited by Stocker, T., Qin, D., Plattner, G.-K., Tignor, M., Allen, S., Boschung, J., Nauels, A., Xia, Y., Bex, V., and Midgley, P., book section 2, p. 159–254, Cambridge University Press, Cambridge, United Kingdom and New York, NY, USA, doi:10.1017/CBO9781107415324.008, [www.climatechange2013.org](http://www.climatechange2013.org), 2013.
- 285 Hase, F., Hannigan, J., Coffey, M., Goldman, A., Höpfner, M., Jones, N., Rinsland, C., and  
290 Wood, S.: Intercomparison of retrieval codes used for the analysis of high-resolution, ground-

- based FTIR measurements, *Journal of Quantitative Spectroscopy and Radiative Transfer*, 87, 25 – 52, doi:<http://dx.doi.org/10.1016/j.jqsrt.2003.12.008>, <http://www.sciencedirect.com/science/article/pii/S0022407303003765>, 2004.
- 295 Kiel, M., Wunch, D., Wennberg, P. O., Toon, G. C., Hase, F., and Blumenstock, T.: Improved retrieval of gas abundances from near-infrared solar FTIR spectra measured at the Karlsruhe TCCON station, *Atmospheric Measurement Techniques*, 9, 669–682, doi:10.5194/amt-9-669-2016, <http://www.atmos-meas-tech.net/9/669/2016/>, 2016.
- 300 Kulawik, S. S., Jones, D. B. A., Nassar, R., Irion, F. W., Worden, J. R., Bowman, K. W., Machida, T., Matsueda, H., Sawa, Y., Biraud, S. C., Fischer, M. L., and Jacobson, A. R.: Characterization of Tropospheric Emission Spectrometer (TES) CO<sub>2</sub> for carbon cycle science, *Atmospheric Chemistry and Physics*, 10, 5601–5623, doi:10.5194/acp-10-5601-2010, <http://www.atmos-chem-phys.net/10/5601/2010/>, 2010.
- 305 Kuze, A., Suto, H., Nakajima, M., and Hamazaki, T.: Thermal and near infrared sensor for carbon observation Fourier-transform spectrometer on the Greenhouse Gases Observing Satellite for greenhouse gases monitoring, *Appl. Opt.*, 48, 6716–6733, doi:10.1364/AO.48.006716, <http://ao.osa.org/abstract.cfm?URI=ao-48-35-6716>, 2009.
- Myhre, G., Shindell, D., Bréon, F.-M., Collins, W., Fuglestedt, J., Huang, J., Koch, D., Lamarque, J.-F., Lee, D., Mendoza, B., Nakajima, T., Robock, A., Stephens, G., Takemura, T., and Zhang, H.: Anthropogenic and Natural Radiative Forcing, in: *Climate Change 2013: The Physical Science Basis. Contribution of Working Group I to the Fifth Assessment Report of the Intergovernmental Panel on Climate Change*, edited by Stocker, T., Qin, D., Plattner, G.-K., Tignor, M., Allen, S., Boschung, J., Nauels, A., Xia, Y., Bex, V., and Midgley, P., book section 8, p. 659–740, Cambridge University Press, Cambridge, United Kingdom and New York, NY, USA, doi:10.1017/CBO9781107415324.018, [www.climatechange2013.org](http://www.climatechange2013.org), 2013.
- 310 Olsen, S. C. and Randerson, J. T.: Differences between surface and column atmospheric CO<sub>2</sub> and implications for carbon cycle research, *Journal of Geophysical Research: Atmospheres*, 109, doi:10.1029/2003JD003968, <http://dx.doi.org/10.1029/2003JD003968>, d02301, 2004.
- 315 Rayner, P. J. and O’Brien, D. M.: The utility of remotely sensed CO<sub>2</sub> concentration data in surface source inversions, *Geophysical Research Letters*, 28, 175–178, doi:10.1029/2000GL011912, <http://dx.doi.org/10.1029/2000GL011912>, 2001.
- 320 Reuter, M., Bovensmann, H., Buchwitz, M., Burrows, J. P., Connor, B. J., Deutscher, N. M., Griffith, D. W. T., Heymann, J., Keppel-Aleks, G., Messerschmidt, J., Notholt, J., Petri, C., Robinson, J., Schneising, O., Sherlock, V., Velasco, V., Warneke, T., Wennberg, P. O., and Wunch, D.: Retrieval of atmospheric CO<sub>2</sub> with enhanced accuracy and precision from SCIAMACHY: Validation with FTS measurements and comparison with model results, *Journal of Geophysical Research: Atmospheres*, 116, doi:10.1029/2010JD015047, <http://dx.doi.org/10.1029/2010JD015047>, d04301, 2011.
- 325 TCCON-Wiki: TCCON Requirements, [https://tcon-wiki.caltech.edu/Network\\_Policy/Data\\_Protocol](https://tcon-wiki.caltech.edu/Network_Policy/Data_Protocol), 2010.
- Velasco, E., Pressley, S., Allwine, E., Westberg, H., and Lamb, B.: Measurements of {CO<sub>2</sub>} fluxes from the Mexico City urban landscape, *Atmospheric Environment*, 39, 7433 – 7446, doi:<http://dx.doi.org/10.1016/j.atmosenv.2005.08.038>, <http://www.sciencedirect.com/science/article/pii/S1352231005008307>, 2005.

**Table 1.** Microwindows and interfering species used for CO<sub>2</sub> and O<sub>2</sub> retrievals.

	Microwindows (cm <sup>-1</sup> )	Interfering species
CO <sub>2</sub>	6180.0 – 6260.0, 6310.0 – 6380.0	H <sub>2</sub> O, CH <sub>4</sub>
O <sub>2</sub>	7765.0 – 8005.0	H <sub>2</sub> O, CO <sub>2</sub>

- 330 Velasco, E., Pressley, S., Grivicke, R., Allwine, E., Coons, T., Foster, W., Jobson, B. T., Westberg, H., Ramos, R., Hernández, F., Molina, L. T., and Lamb, B.: Eddy covariance flux measurements of pollutant gases in urban Mexico City, *Atmospheric Chemistry and Physics*, 9, 7325–7342, doi:10.5194/acp-9-7325-2009, <http://www.atmos-chem-phys.net/9/7325/2009/>, 2009.
- WMO: The Global Atmospheric Watch Programme: 17th WMO/IAEA Meeting on Carbon Dioxide, Other  
335 Greenhouse Gases and Related Tracers Measurement Techniques (GGMT-2013), Beijing, China, 10-13 June 2013, GAW Report No. 213, World Meteorological Organization, Geneva, Switzerland, 2014, 2014.
- Wunch, D., Toon, G. C., Blavier, J.-F. L., Washenfelder, R. A., Notholt, J., Connor, B. J., Griffith, D. W. T., Sherlock, V., and Wennberg, P. O.: The Total Carbon Column Observing Network, *Philosophical Transactions of the Royal Society of London A: Mathematical, Physical and Engineering Sciences*, 369, 2087–2112,  
340 doi:10.1098/rsta.2010.0240, <http://rsta.royalsocietypublishing.org/content/369/1943/2087>, 2011.
- Wunch, D., Wennberg, P. O., Messerschmidt, J., Parazoo, N. C., Toon, G. C., Deutscher, N. M., Keppel-Aleks, G., Roehl, C. M., Randerson, J. T., Warneke, T., and Notholt, J.: The covariation of Northern Hemisphere summertime CO<sub>2</sub> with surface temperature in boreal regions, *Atmospheric Chemistry and Physics*, 13, 9447–9459, doi:10.5194/acp-13-9447-2013, <http://www.atmos-chem-phys.net/13/9447/2013/>, 2013.
- 345 Wunch, D., Wennberg, P. O., Osterman, G., Fisher, B., Naylor, B., Roehl, C. M., O’Dell, C., Mandrake, L., Viatte, C., Griffith, D. W., Deutscher, N. M., Velasco, V. A., Notholt, J., Warneke, T., Petri, C., De Maziere, M., Sha, M. K., Sussmann, R., Rettinger, M., Pollard, D., Robinson, J., Morino, I., Uchino, O., Hase, F., Blumenstock, T., Kiel, M., Feist, D. G., Arnold, S. G., Strong, K., Mendonca, J., Kivi, R., Heikkinen, P., Iraci, L., Podolske, J., Hillyard, P. W., Kawakami, S., Dubey, M. K., Parker, H. A., Sepulveda, E., Rodriguez,  
350 O. E. G., Te, Y., Jeseck, P., Gunson, M. R., Crisp, D., and Eldering, A.: Comparisons of the Orbiting Carbon Observatory-2 (OCO-2) X<sub>CO<sub>2</sub></sub> measurements with TCCON, *Atmospheric Measurement Techniques Discussions*, 2016, 1–45, doi:10.5194/amt-2016-227, <http://www.atmos-meas-tech-discuss.net/amt-2016-227/>, 2016.

**Table 2.** Error sources used in the error estimation, the second column gives the uncertainty used and the third the statistical (Stat) and systematic (Sys) contributions of each source in percentage.

Error Source	Uncertainty	Stat / Sys [%]
Baseline (offset / channelling)	0.1% / 0.2%	50 / 50
ILS (mod. eff. / phase error)	2% / 0.01 rad	50 / 50
Line of sight	0.001 rad	90 / 10
Solar lines (intensity / scale)	1% / $1e10^{-6}$	80 / 20
Temperature	1, 2 & 5 K	70 / 30
Spectroscopic parameters ( $S / \gamma$ )	2% / 5%	0 / 100
Measurement noise	-	100 / 0

**Table 3.** Mean ensemble values of the statistical (Stat) and systematic (Sys) errors for 20° and 70° SZA (given in %), in CO<sub>2</sub> columns due to the assumed error sources of Table 2.

CO <sub>2</sub>	SZA = 20°				SZA = 70°			
	KBr		CaF <sub>2</sub>		KBr		CaF <sub>2</sub>	
	Stat	Sys	Stat	Sys	Stat	Sys	Stat	Sys
Baseline	0.082	0.082	0.081	0.081	0.085	0.085	0.085	0.085
ILS	0.073	0.073	0.076	0.076	0.043	0.043	0.043	0.043
LOS	0.031	0.0035	0.031	0.0034	0.24	0.026	0.24	0.026
Solar lines	0.0071	0.0018	0.0092	0.0023	0.0065	0.0016	0.0082	0.0020
Temperature	0.019	0.0081	0.012	0.0053	0.031	0.013	0.032	0.014
Spectroscopy	—	2.13	—	2.16	—	2.13	—	2.13
Noise	0.039	—	0.047	—	0.037	—	0.035	—
TOTAL	0.12	2.14	0.13	2.16	0.26	2.13	0.26	2.13

**Table 4.** Mean ensemble values of the statistical (Stat) and systematic (Sys) errors for 20° and 70° (given in %), in O<sub>2</sub> columns due to the assumed error sources of Table 2.

O <sub>2</sub>	SZA = 20°				SZA = 70°			
	KBr		CaF <sub>2</sub>		KBr		CaF <sub>2</sub>	
	Stat	Sys	Stat	Sys	Stat	Sys	Stat	Sys
Baseline	0.090	0.090	0.087	0.087	0.089	0.089	0.090	0.090
ILS	0.060	0.060	0.059	0.059	0.032	0.032	0.032	0.032
LOS	0.031	0.0034	0.030	0.0033	0.22	0.025	0.22	0.024
Solar lines	0.0077	0.0019	0.0077	0.0019	0.0044	0.0011	0.0047	0.0012
Temperature	0.029	0.012	0.033	0.014	0.031	0.013	0.032	0.014
Spectroscopy	—	2.12	—	2.10	—	2.89	—	2.90
Noise	0.046	—	0.063	—	0.074	—	0.053	—
TOTAL	0.13	2.12	0.13	2.10	0.25	2.89	0.25	2.90

**Table 5.** Mean precision, noise and correlation errors (given in %) for both ensembles, of 2,093 measurements each, using KBr and CaF<sub>2</sub> beamsplitters. The  $X_{CO_2}$  precision is the root-sum-square of the noise errors of CO<sub>2</sub> and O<sub>2</sub>.

	$\sigma_{CO_2}$	$\sigma_{O_2}$	$\sigma^{Correlated}$	$\sigma_{CO_2}^{Noise}$	$\sigma_{O_2}^{Noise}$	$\sigma_{XCO_2}$
KBr	0.072 ± 0.0041	0.098 ± 0.0042	0.055 ± 0.0055	0.047 ± 0.0065	0.082 ± 0.0037	0.094 ± 0.0033
CaF <sub>2</sub>	0.078 ± 0.0046	0.090 ± 0.0037	0.065 ± 0.0031	0.043 ± 0.0048	0.062 ± 0.0033	0.075 ± 0.0022

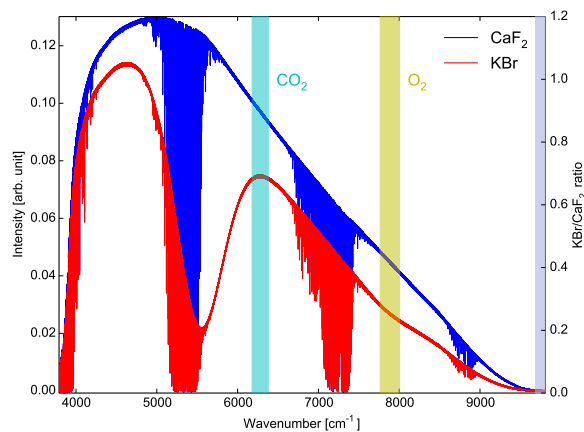


**Figure 1.** Spectra of a near infrared (NIR) lamp measured with KBr (red) and CaF<sub>2</sub> (blue) beamsplitters, the spectral regions where the CO<sub>2</sub> and O<sub>2</sub> target gases are retrieved are shown in cyan and yellow, respectively. The KBr/CaF<sub>2</sub> lamp intensity ratio, as shown in grey, is smooth at the target regions and is lower for O<sub>2</sub> (the gas which presents larger error differences among beamsplitters).

**Table 6.** Mean values of  $X_{CO_2}$ ,  $CO_2$  and  $O_2$  and the bias obtained for each of them using the beamsplitters ensembles. For  $X_{CO_2}$ , the Mauna Loa Observatory (MLO) was used and for  $O_2$  the dry pressure column was calculated and multiplied by 0.2095. The bias of  $CO_2$  was obtained from Eq. 4.

	KBr	CaF <sub>2</sub>
$X_{CO_2}$		
Coincidences	189	174
Mean Value FTIR [ppm]	$396.07 \pm 0.12$	$396.68 \pm 0.14$
Mean Value MLO [ppm]	$399.82 \pm 0.14$	$402.04 \pm 0.20$
Mean Difference [ppm]	$-3.75 \pm 0.077$	$-5.36 \pm 0.11$
Bias (KBr-CaF <sub>2</sub> ) [ppm]	$+0.56 \pm 0.25$ ( $+0.14 \pm 0.064$ %)	
$O_2$		
Coincidences	100	110
Mean Value FTIR [ $10^{24}$ molec $cm^{-2}$ ]	$2.90 \pm 0.00089$	$2.90 \pm 0.00077$
Mean Value dry pressure column [ $10^{24}$ molec $cm^{-2}$ ]	$2.82 \pm 0.00055$	$2.82 \pm 0.00046$
Mean Difference [ $10^{24}$ molec $cm^{-2}$ ]	$0.078 \pm 0.00050$	$0.081 \pm 0.00051$
Bias (KBr-CaF <sub>2</sub> ) [ $10^{24}$ molec $cm^{-2}$ ]	$-0.0050 \pm 0.00083$ ( $-0.17 \pm 0.029$ %)	
$CO_2$		
Mean Value FTIR [ $10^{24}$ molec $cm^{-2}$ ]	$5.49 \pm 0.00034$	$5.50 \pm 0.00031$
Bias [ $10^{24}$ molec $cm^{-2}$ ]	$-0.0016 \pm 0.0039$ ( $-0.030 \pm 0.070$ %)	

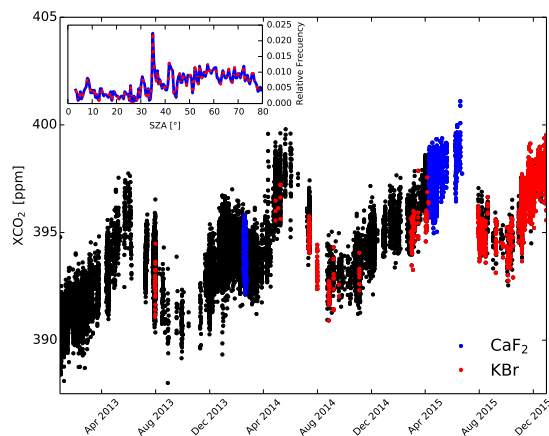


**Figure 2.** Time series of the  $X_{CO_2}$  data set from Altzomoni site (black points) with the elements of the KBr (red points) and the CaF<sub>2</sub> (blue points) ensembles. The inset plot show the SZA distribution of both ensembles.

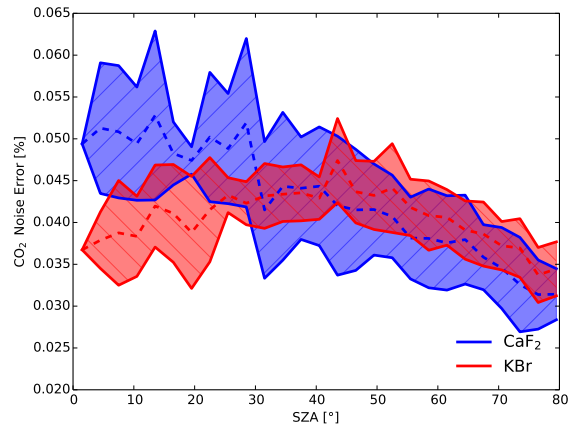


**Figure 3.** Mean noise error from PROFFIT for CO<sub>2</sub> total column in function of SZA.

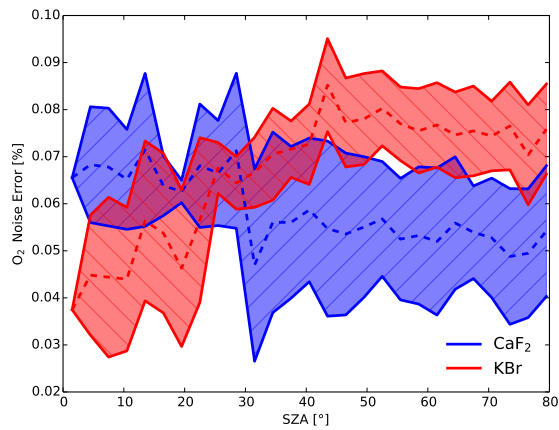


**Figure 4.** Mean noise error from PROFFIT for O<sub>2</sub> total column in function of SZA.

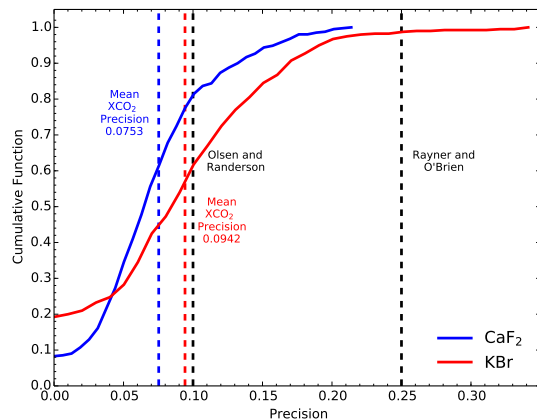


**Figure 5.** Cumulative function of  $X_{CO_2}$  precision for both beamsplitters with the blue and red dashed lines denoting the precision values from Table 5 obtained from the [top-down Section 3.2](#) approach. The black lines depict the existing [precision-precision](#) goals for  $CO_2$  found in the literature.

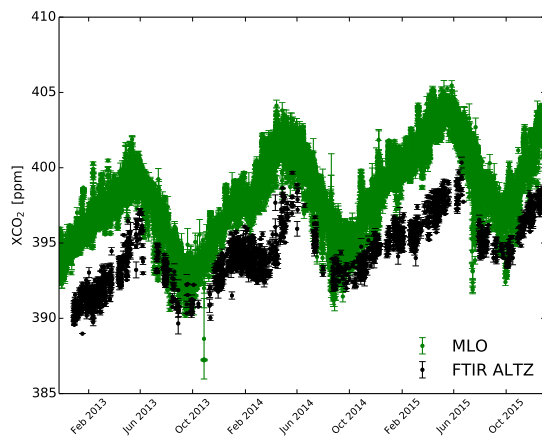


**Figure 6.** Hourly means of Altzomoni  $X_{CO_2}$  (FTIR ALTZ, black points) and Mauna Loa Observatory in situ  $CO_2$  (MLO, green points)

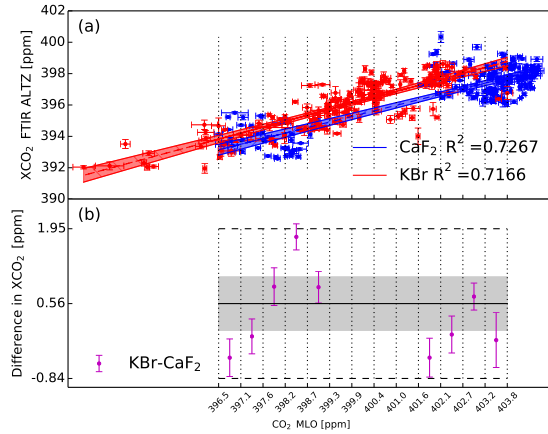


**Figure 7.** Upper panel (a) shows the coincidences between the hourly means of the  $X_{CO_2}$  from the KBr (red) and CaF<sub>2</sub> (blue) ensembles and the CO<sub>2</sub> from the Mauna Loa Observatory (MLO) data set with a linear regression of the two sets with the shaded area representing a 95% confidence interval. Lower panel (b) shows the difference of means of KBr and CaF<sub>2</sub> (purple points) for each bin (vertical lines) in a Bland-Altman plot, with the black dashed lines showing the standard deviation of all points. The black solid line represents the bias and the shaded area the standard error of the bias, both reported in Table 6.

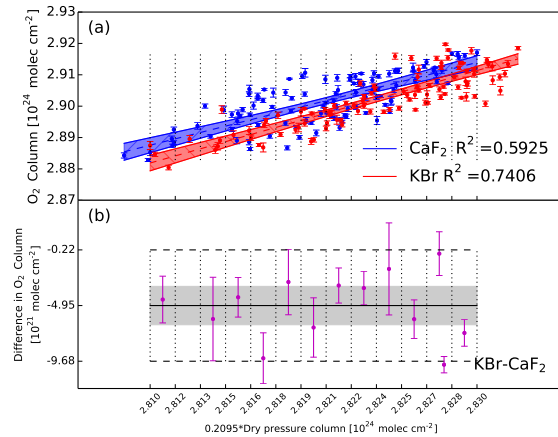


**Figure 8.** Upper panel (a) shows the coincidences between the hourly means of the O<sub>2</sub> from the KBr (red) and CaF<sub>2</sub> (blue) ensembles and the O<sub>2</sub> column obtained from the dry pressure column with a linear regression of the two sets with the shaded area representing a 95% confidence interval. Lower panel (b) shows the difference of means of KBr and CaF<sub>2</sub> (purple points) for each bin (vertical lines) in a Bland-Altman plot, with the black dashed lines showing the standard deviation of all points. The black solid line represents the bias and the shaded area the standard error of the bias, both reported in Table 6.

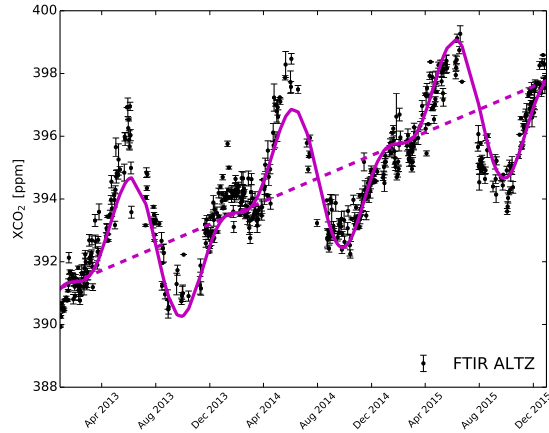


**Figure 9.** Daily means of the  $X_{CO_2}$  data set from the Alzomoni site (black points). The purple solid line is a curve adjusted to the series (see text) with a linear term, represented by the dashed line, of 2.2 ppm/year which is the trend for this 3-year period.

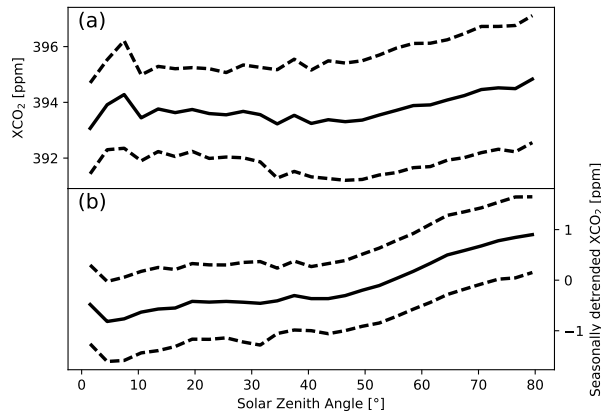


**Figure 10.** Detrended diurnal cycle of the  $X_{CO_2}$  data set from the Alzomoni site (black line) with detrended diurnal cycle as a function of MLO solar zenith angle. Lower panel (green line) shows the seasonally detrended  $X_{CO_2}$  using the coefficients obtained for the Eq. The time of each measurement was converted to true solar time. Each bin represents the average of the hour marked containing data from 0 to 59 minutes. The solid lines represent mean values and the dashed lines standard deviations.